



DOI: **10.5958/2249-7137.2021.02299.0**

STUDY AND ANALYSIS OF THE CONVERSION PROCESS OF PROPANO-BUTANE MIXTURE IN HIGH SILICATE ZEOLITIC CATALYSTS OF DIFFERENT SILICATE MODULES AND DIFFERENT STRUCTURES

Javharov Jonibek Joraqul oqli*; **Xolliyev Shamsiddin Xudoyberdiyevich****;
Tursunova Nargiza Samariddinovna***

^{1,3}Samarkand State University,
UZBEKISTAN

ABSTRACT

The catalytic aromatization reaction of the propane-butane fraction was carried out on a mesoporous catalyst containing Pt, Zn, Ga and Cd / N-ZSM-5 under the following optimal conditions: Catalytic conversion of propane-butane alkanes at atmospheric pressure went. The reaction was carried out under conditions of temperature 723 to 873 K and volumetric velocity of the raw material from 50 to 150 h. The conversion reaction of a mixture of alkanes containing C₂H₆ = 2.2; C₃H₈ = 73.7; N-S4N10 = 24.1%. In high-silicate zeolite catalysts with the structure ZSM-5 ($\frac{[SiO]}{[Al]} \frac{O_3}{O_3} = 30, 50, 70 \text{ and } 100$) and ZSM-11 ($\frac{[SiO]}{[Al]} \frac{O_3}{O_3} = 100$), the catalytic contacts the relationship between their structural and acidic characteristics and their activity in the formation of conversion products was studied. Depending on the silicate modulus, it was found that the conversion rate of the alkane mixture S₂-S₄ varies and is 96% at $[T = 823K \text{ and } v = 100 \text{ s}]^{-1}$. The distribution curves of the volume of the pores to the equivalent diameters were compared. The largest part of the pores is 13 to 20 diametri in diameter. YuK zeolites also have medium (25-50 Å) and large (50-90 Å) mesocytes. The distribution corresponds to 32–35 bo'yicha along the curves. The sizes of the largest mesocytes for these catalysts vary - from 63 to 80 Å.

KEYWORDS: Propane, Butane, Chromatographic Analysis, Volumetric Velocity, High Silicon Zeolite, Catalyst, Texture Characteristic, Meso Porosity, Acidity Center, IR Spectrum, Adsorption-Desorption Of Benzene, Adsorption Of Ammonia, Propane Adsorption Isotherms, Propane Adsorbers.

INTRODUCTION

The most efficient way to process propane-butane fractions is to chemically process them to obtain aromatic hydrocarbons. Aromatic hydrocarbons are important primary products in the main organic synthesis industry. At present, aromatic hydrocarbons are processed into liquid products of oil catalytic reforming and pyrolysis processes. Changes in the petrochemical complex raw material base are leading to a shortage of these hydrocarbons. Therefore, the search for alternative energy sources to replace petroleum products to obtain aromatic hydrocarbons remains an important task. Alternative sources today are natural gas and petroleum gases. A number of scientists are conducting research on the catalytic synthesis of aromatic hydrocarbons [1-5]. In this reaction, high-silicon zeolites containing Zn, Zr, and Pt have high catalytic activity [2,5,6]. The disadvantage of the catalytic interaction of these systems is that the reaction produces a certain amount of methane and high molecular weight aromatic hydrocarbons (naphthalene, alkyl naphthalene). As a result, the stable service life of catalysts is reduced.

Currently, scientists around the world are interested in the process of obtaining aromatic hydrocarbons from natural gas and petroleum gases in one step.

Zeolite catalysts, especially those modified with metals and metal oxides, are widely used in petroleum refining and petrochemistry [7-11]. The traditional method of obtaining such catalytic systems is to absorb the metal salts into the zeolite and gradually decompose the introduced precursor [12 - 19]. However, in this method, the modifiers are not evenly distributed throughout the entire volume of the zeolite, but are localized on the surface of the zeolite crystals. This reduces the performance efficiency of the catalyst. However, the acidity centers of the catalyst also play an important role in the catalytic activity of the catalytic system. Hydrothermal synthesis is important in ensuring the isomorphic exchange of aluminum or silicon in the zeolite crystal lattice for modifiers. The acidity and texture characteristics of the catalyst are improved due to isomorphic exchange in hydrothermal synthesis. This paper presents the results of the study of the kinetic laws of the catalytic aromatization reaction of propane in the catalyst Pt, Zn, Ga and Cd / N- ZSM-5.

A large value of selectivity for aromatic hydrocarbons was obtained by adding Zn⁽²⁺⁾ cations. In [120, 121], the catalytic properties of Zn / N-ZSM-5 samples prepared by ion exchange and pentacyl in the first-burned form Zn⁽²⁺⁾ during propane conversion were compared. , while the selectivity of aromatization doubles. During the modification of the propane and butane mixture, 5% Zn / N-ZSM-5, in which case $S_{ar} = 65.1\%$. Synthesis of high silica-zeolite catalysts (YUKs) was carried out in steel autoclaves at a temperature of 448 K for 6 days. The initial reaction mixture was prepared and mixed by adding an aqueous solution of aluminum salts $Al_2(SO_4)_3 \cdot xH_2O$ analytical and hexamethylenediamine to the liquid glass (29% SiO₂; 9% Na₂O; 62% H₂O). The pH of the reaction mixture was adjusted by the addition of HNO₃ solution. YUKTs powder (1.5 g) was added to the reaction mixture.

The aim of this work is to obtain a mesocellular catalyst containing Zn, Ga and Cd / N- ZSM-5, to study its physicochemical and catalytic properties in the aromatization reaction of propane.

EXPERIMENTAL PART

A mixture of gases: ethane - 2.2%, propane - 73.7%, N -butane - 24.1% by weight, the lower alkanes were used as raw materials for the conversion reaction. The studies were performed in a

reactor with a flow rate of 5 cm^3 at atmospheric pressure. The reactor was heated using a quartz furnace located in a thermostat. The temperature in the quartz furnace was measured with VRT-3. After passing through the catalyst mixture, the reaction products and the remaining unconverted raw material go to the water condenser for condensation. The liquid reaction products are placed in a Dewar tube filled with ice and collected in a collector. The volume of exhaust gases was measured using a GSB-400 gas meter, and a gas sample was taken for analysis using a metering valve. Catalytic conversion of low molecular weight alkanes was carried out under atmospheric pressure at a reaction temperature of 723 to 873 K and a bulk rate of the raw material from 50 to 150 h. The reaction products were obtained for analysis after 30 min. VTK fractions, C₉₊ hydrocarbons, naphthalene and methylnaphthalene. C₂-C₄ alkane conversion products were analyzed using gas chromatography on a chromium chromatograph with a thermal conductivity detector. Analysis of gaseous products - in a column filled with Al₂O₃ (0.25-0.5 mm, column length - 4 m, inner diameter - 3 mm), in the temperature programming mode from 298 to 423 K, with heater, speed 12 degrees / min. Carrier (He) gas velocity - $50 \text{ cm}^3 / \text{min}$. The chromatogram of gaseous products is shown in Figure 2.5. Liquid hydrocarbons were analyzed on a S₂₊ base at a temperature programming mode of 352 to 473 K at a rate of $12 \text{ }^\circ\text{C} / \text{min}$, and then at an isothermal mode at 473 K on a PFMS-4 stationary phase packed column. The chromatogram of gaseous products is shown in Figure 2.5. ZSM-5 and $[\text{SiO}]_2 / [\text{Al}]_2 \text{O}_3 = 50$ structured YuK zeolite were used as the basis for catalytic studies. Modification of zeolite was carried out by impregnation with solutions of salts and acids of the corresponding metals, as well as by obtaining five modified catalysts with boric acid: 5% V-VKTs; 5% Mn- VKTs; 1% Rt- VKTs; 1% Rt - 5% Mn / VKTs; 1% Pt - 5% Sn / VKTs. The catalytic activity of the obtained zeolite catalysts was studied in units of flow at atmospheric pressure. During the experiments, the effect of process temperature and voltmetric consumption rate on the conversion rate and the selectivity of aromatic hydrocarbon formation was studied.

Additives of various metals - Zn, Pd, Mo, W and Zn - increase the service life of pentacyl catalysts by 2-10 times []. Cadmium ions are added to zeolite to activate aromatization activity and selectivity. At $T = 873 \text{ K}$ $v = 110 \text{ Cd} / \text{N-ZSM-5}$, the selectivity in the propane and butane mixture converts to a mixture of aromatic hydrocarbons at 64.1%, with a conversion of 80–84%. Metal-containing zeolite catalysts were prepared by soaking zeolite in an N-shaped salt or with solutions of certain salts or acids. A certain amount of zeolite was mixed with a certain amount of modifying solution, and the mixture was kept for two hours with constant stirring. The mixture was then immersed in a water bath. After that, the sample obtained is dried at 383 K for 6 hours and baked in a muffle furnace at 793 K for 8 hours. Thus 1% Pt-H / ZSM-5 with the following content; 5% B- H / ZSM-5; 5% Mn - H / ZSM-5, catalysts were obtained: (as a modifier we used solutions of H₄ PtCl₆, boric acid H₃ [BO]₃ and manganese nitrate salt $[\text{Mn}(\text{NO})_3]_2 \times 6 \text{ H}_2 \text{O}$. The second catalyst was 5% Mn with 1% 1% Pt-H / ZSM-5 and 5% Sn 1% Pt-H / ZSM-5. Platinum-modified zeolite catalysts were activated prior to the experiment at atmospheric oxygen flow at 573 K for 3 h and then at hydrogen flow at 793 K for 4 h.

IC spectroscopy and X-ray analysis were performed using physicochemical methods to study YuKTs: IR spectra of the studied zeolites (Figure 2.1) were recorded on a UR-20 spectrophotometer in the mid-wavelength part of the spectrum at 400-2000 cm⁻¹, where the

absorption ranges were AlO_4 of the base. $[\text{And SiO}]_4$ are the principal oscillations of the tetrahedron. To do this, 1-2 mg of the sample and 400 mgKBr of potassium bromide are poured into a special ring placed in a mold, then the sample ring is inserted into the holder and placed on a spectrophotometer. Absorption lines in the observed spectrum can be divided into 2 types of oscillations.

The first type of oscillations corresponds to oscillations at 1120 cm^{-1} , 820 cm^{-1} and 470 cm^{-1} found in the whole zeolite spectrum. The strong absorption range at the apex of 1120 cm^{-1} is related to the antisymmetric oscillations of the tetrahedron $[\text{SiO}]_4$, while the 820 cm^{-1} length 3104 cm^{-1} tetrahedra represents the oscillations mainly involved. - The presence of strong absorption lines 1300-900, 820, 400-600 cm^{-1} in the region of all spectra testifies to the fact that all samples belong to zeolites.

- that all tested specimens belong to the ZSM constructive type, since all IR spectra obtained include the absorption peaks line 560 cm^{-1} . the ratio of the optical absorption ranges to 560 and 460 cm^{-1} (I_{560} / I_{460}) [173], the crystallization rate of all studied samples was calculated: $\text{SiO}_2 / \text{Al}_2\text{O}_3$ (3) for ZSM-5 zeolites with a ratio of 30, 50, 70, 100; crystallinity level 89, 2, respectively; 93.3; 91.5; 88.2% are equal. For the ZSM-11 catalyst ($\text{SiO}_2 / \text{Al}_2\text{O}_3 = 100$), the crystallization rate is 88.1%. There are no significant differences in IR spectra for ZSM-5 and ZSM-11 zeolites; therefore X-ray analyzes were performed to improve the structure of the zeolites in detail. X-ray analyzes (Mo-anode, Ni-filter) were performed using Dron-3. Processing of the diffraction lines of zeolites was carried out by determining the distances and intensities of the lines (peaks) of the studied zeolite sample by comparing the distance lines between the planes (their position and relative intensity) with the corresponding line sample.

Thermal desorption measurements were set by programming heating the sample and recording the signal from the detector on a flat potentiometer sheet PDP 4-002 (or on the lines of the KSP-4 potentiometer). The chromatographic version of thermal desorption is that the catalyst sample, which is a molecule of a previously adsorbed substance, is heated at a certain constant rate in a stream of carrier gas and it passes through a detector. During desorption, the detector signal is recorded on a diagram sheet of the potentiometer.

A test sample of 0.3–0.5 g was placed in a quartz reactor and purified with carrier gas (He) at 373 K for 2 h. Carrier gas velocity 170 $\text{cm}^{-1} / \text{min}$. The sample reactor was then cooled to 373 K and ammonia adsorption was performed until the sample was completely saturated. With the sample, the reactor was cooled to 298 K. Thermal desorption of NH_3 was carried out at a rate of 170 $\text{cm}^{-1} / \text{min}$ of carrier gas (helium) with a programmed heating of the sample at -10 degrees / min.

After device inspection, the adsorbent (35-45 mg) was trained at 723 K in vacuum to remove contaminants for 6 h. The catalyst thus transferred is considered ready for adsorption measurements. Benzene and propane were used as adsorbates. Adsorption of benzene was studied at 293 K. The adsorption value is calculated according to the following formula.

$$a = (D \times f) / m$$

a = mmol / g adsorption amount;

f = spiral constant mmol / mm;

DI = elongation of the spiral, mm;

m = sample weight, g

The size distribution of the pores was calculated from the desorption networks of benzene adsorption isotherms using the Thomson-Kelvin equation:

$$d_{\text{ekv}} = (4\sigma V_m) / (RT \lg P_s / P)$$

d_ekv = equivalent pore diameter. Å;

σ is the surface tension of benzene, din / cm;

V_m - molar volume of liquid, cm³ / mol;

P - equilibrium pressure, mm.Hg

Saturated vapor pressure of P_s-adsorbate, mm of mercury column

Changes in the structure of micropores were determined by the theory of volumetric filling according to the Dubinina-Radushkevich equation [71]:

$$\lg a = \lg \frac{W_0}{V_M} - 0,434 \frac{BT^3}{\beta^3} \left(\lg \frac{P_s}{P} \right)^3$$

a is the value of adsorption at temperature and equilibrium pressure R-mol / g

W_0 - total volume of micropores, cm³ / g;

V_M is the molar volume of the adsorbate, mol / cm³

T is the temperature of the experiment, in K;

R is the equilibrium pressure of the adsorbate, mm of mercury;

P_s is the saturated vapor pressure of the adsorbate, mm of mercury

b is the proximity coefficient;

The B-parameter reflects the size of the micro-pores in the sample, the smaller the micro-pores in the adsorbent, the lower the B-value.

The B-coefficient is directly related to the adsorption energy (E):

$$B = (2,303 R/E)^3$$

When constructing the dependencies in the coordinates $\lg a - (\lg (P_s / P))^3$, B-parameters for the studied zeolite catalysts were determined.

The total volume of the adsorption gap (W_s) and the volume of the micro-pores (V_ (m.g.)) Were determined from the experimental adsorption isotherm [23, 180]:

$$W_s = a_s x V_m; V_ (p.p) = W_s - V_ (m.g.); M_ (m.g) = a_0 x V_m;$$

a_s-adsorption value $P_s / P_s = 1$, such as mmol / g;

V_m is the volume of millimol adsorbate in the liquid state, cm³ / mmol;

a_0 is the value of adsorption at the relative pressure corresponding to the onset of capillary condensation in the transition pores, mmol / g.

$V_-(p,p)$ is the volume of the passing mesentery.

Propane adsorption was performed in the temperature range of 293–393 K.

The adsorption temperature of propane was determined from the adsorption isosters

$$a = \text{const}n, \ln p = -\frac{q}{RT} + B$$

The chemical composition of the sample was analyzed by energy-dispersion spectrometer and radiographic method with a scanning electron microscope.

Acidic, alkaline and thermal activation of bentonite is a common method in obtaining porous sorbents for the synthesis of organic and inorganic substances.

EXPERIMENTAL RESULTS AND THEIR DISCUSSION

It is known from the scientific literature that the catalytic properties of modified catalysts are directly related to their acidic properties. The acidity centers of zeolite catalysts are an important factor in determining their catalytic activity, as such centers are of 2 types. Weak and strong acid centers. The study of the acidic properties of catalysts by the TPD method of ammonia showed that ammonia is adsorbed in two forms on YuK zeolites, indicating the presence of two peaks in the TPD curve (Figure 3.3). Low-temperature peaks in the 393–613 K region indicate desorption of ammonia from weakly acidic centers, and high-temperature peaks in the 613–823 K region indicate strong Brønsted and Lewis acid centers. [1]. The amount of desorbed ammonia in the specified temperature range can serve to measure the number of these and other centers, and the maximum state of the ammonia in the TPD curve and the activation energy of NH_3 desorption ($E_{(a.des)}$) are given in Table 1.1.

It follows from the data presented that with an increase in the silicate modulus of zeolite from 30 to 100, a decrease in the total concentration of acid fields is

observed from 1.08 to 0.38 mmol / g. As the ratio of $[\text{SiO}]_2 / [\text{Al}]_2 \text{O}_3$ increases from 30 to 50, the strength of the acid centers increases.

Катализатор	Максимал ҳарорат К		десорбланган аммиак микдори, ммол / г			NH ₃ нинг десорбция фаоллашуви энергияси, кЖ / мол	
	1	2	1	2	1+2	1	2
ZSM – 5 $\text{SiO}_2/\text{Al}_2\text{O}_3$							
1. M=30	448	688	0,67	0,41	1,08	28	108
2. M=50	493	708	0,41	0,33	0,74	80	150
3. M=70	473	703	0,38	0,23	0,61	25	115
4. M=100	473	698	0,20	0,18	0,38	30	123
5. ZSM – 11	453	683	0,17	0,15	0,32	24	122

Table 1.1. Thermal desorption of ammonia in high silica zeolite catalysts (sample heating rate 10 degrees / min)

The catalytic properties of TsSK were studied in a unit of catalytic bed flow with atmospheric pressure, temperature 673–873 K, and volumetric velocity of the raw material 150 s⁻¹. A 70-module ZSM-5 type zeolite sample was used for the study. The structure of the original zeolite was modified by the method of mechanical-chemical activation in a spherical vibrating mill for 24 h and by the introduction of amorphous matrices into the mechanized zeolite to obtain three CSKs:

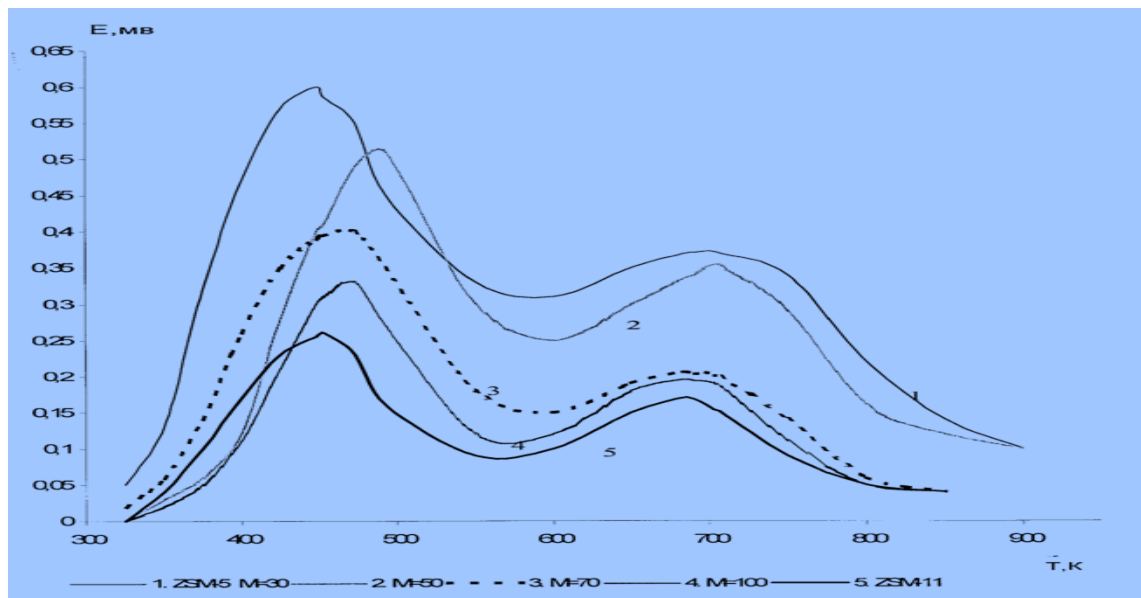


Figure 3.3

Thermal desorption spectra of ammonia adsorbed at 373K in zeolites with different $[\text{SiO}]_2 / [\text{Al}]_2 \text{O}_3$ ratios.

Theoretical calculations of cluster quantum chemical models, as well as data obtained using IR spectroscopy and NMR [40, 45], showed that three major types of hydroxyl groups represent the presence of zeolites in large pores (one, two, or three aluminum atoms). As the ratio of $[\text{SiO}]_2 / [\text{Al}]_2 \text{O}_3$ increases, the acidity of the bridged hydroxyl groups increases, because as the number of negatively charged alumino-oxygen tetrahedrons in the zeolite lattice decreases, the negative charges of the ON groups decrease, their polarity increases, and their polarity increases. This is confirmed by the results of the strength of the acid fields with an increase in the modulus of the silicate from 30 to 50.

Thermal desorption measurements of acid characteristics of zeolite catalysts 1.2. are given in the table.

катализатор	температура максимумов пиков, К		количество десорбированного аммиака, ммоль/г			энергия активации десорбции аммиака, кДж/моль	
	1	2	1	2	1+2	1	2
1. ВКЦ-1	473	703	0,38	0,23	0,61	25	115
2. ВКЦ-2	473	708	0,35	0,22	0,57	25	131
3. ЦСК-1	458	688	0,29	0,17	0,46	30	105
4. ЦСК-2	483	703	0,27	0,20	0,47	41	115
5. ЦСК-3	473	703	0,30	0,20	0,5	28	115
6. Al ₂ O ₃	453	-	0,31	-	0,31	-	-
7. псевдобемит	453	-	0,28	-	0,28	-	-

The original zeolite YuKTs -1 have two different weak and strong acidic centers with activation energy of ammonia desorption - 25 and 115 kJ / mol and acid concentrations - 0.38 and 0.23 mmol / g. As a result of mechanical-chemical purification of zeolite, the total concentration of acidic centers decreases, mainly due to a decrease in the concentration of weak acid centers, while the concentration of strong acidic centers remains practically unchanged.

Table 3.14 Structural properties of catalysts in zeolite

катализатор	ВКЦ-1	ВКЦ-2	ЦСК-1	ЦСК-2	ЦСК-3	Al ₂ O ₃	псевдобемит
адсорбционные измерения							
1. Предельная адсорбционная емкость, W _s , см ³ /г	0,08	0,19	0,31	0,27	0,39	0,38	0,40
2. Объем микропор, V _м , см ³ /г	0,04	0,05	0,07	0,08	0,08	-	-
3. Объем переходных пор, V _{п.п.} , см ³ /г	0,04	0,14	0,24	0,19	0,31	-	-
4. Коэффициенты В, вычисленные из уравнения Дубинина-Радушкевича							
В ₁ ·10 ⁸	0,29	0,69	1,16	1,86	1,32	-	-
В ₂ ·10 ⁸	2,45	2,18	-	-	-	-	-
5. Диаметр мезопор, Å							
1	17	12	-	-	13	13	-
2	32	28	23	23	38	35	25
3	63	-	-	-	50-70	75	-

Figure 3.28 shows the isotherms of propane adsorption in primary pentacyl, mechanized zeolite, CSK, and matrices, of which the maximum value of propane adsorption is observed in the sample YuKTs-1 and is 1.48 mmol / g (at R = 60 mm Hg). Implementation of mechanochemical activation leads to a slight decrease in the propane adsorption capacity of zeolite.

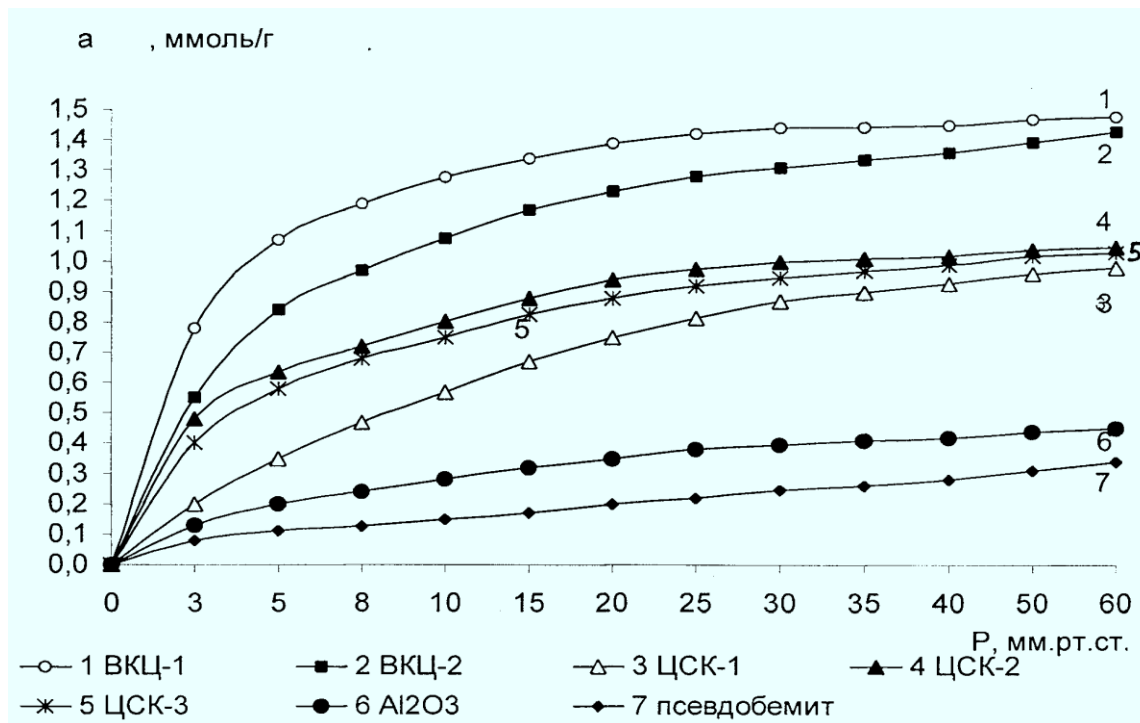


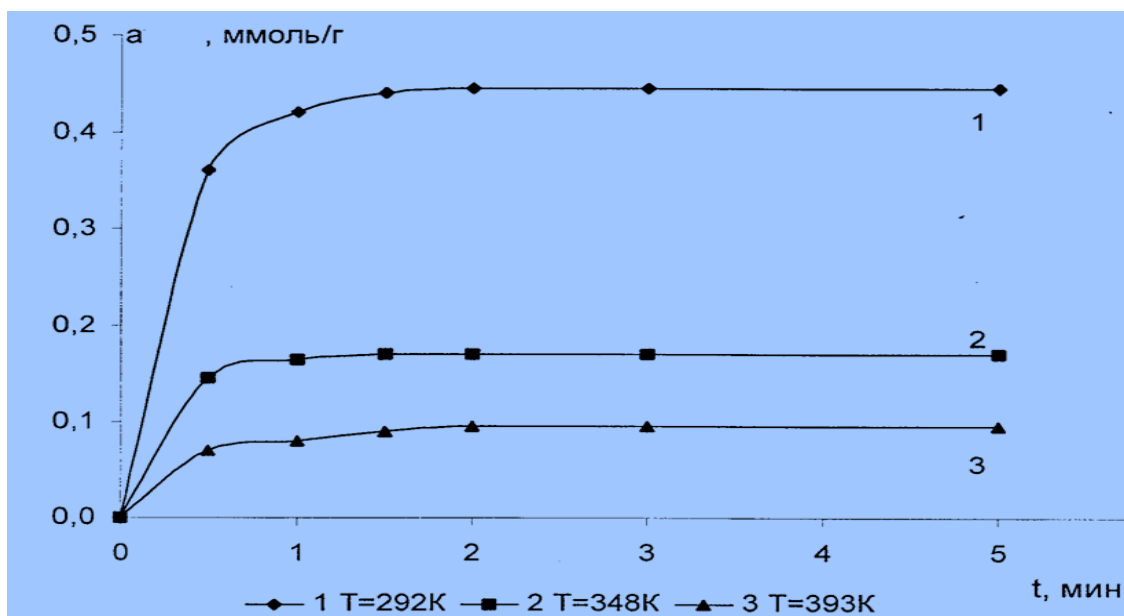
Figure 3.28 Isotherms of propane adsorption in zeolites, CSK and matrices ($T = 292\text{ K}$)

When zeolites are introduced into the matrices, the amount of adsorbed propane is significantly reduced, and the isotherms for mechanically active zeolite (TsSK-2, TsSK-3) zeolite catalysts are higher than the TsSK-1 isotherm. Propane is also absorbed into small amounts of carriers. For the UD Al₂O₃ matrix, the adsorption capacity of propane is high. Figure 3.29 shows the kinetic isotherms of propane adsorption on the TsSK-2 catalyst at $T = 292, 348$ and 393 K .

As can be seen from the figure, an increase in the experimental temperature leads to a decrease in the time required to establish the adsorption equilibrium and a decrease in the amount of adsorbed substance. The same property is retained for all the catalysts studied. The calculation of propane adsorption values on pure zeolite in CSK is based on the rules given in paragraph 3.2. The results of the calculations are shown in Figure 3.30, which means that the value of propane adsorption in zeolite containing CSK is higher than the original YuKTs-1 and YuKTs-2.

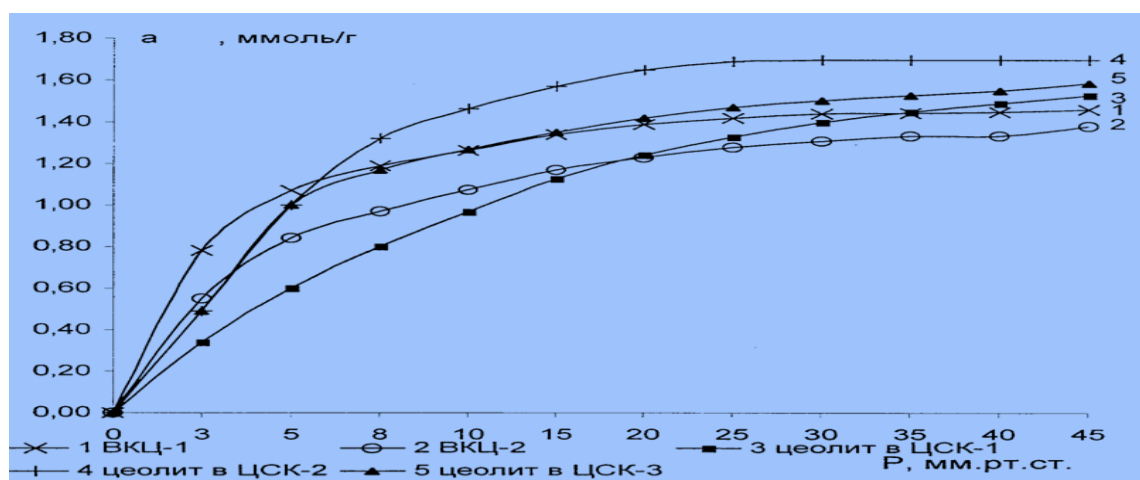
The highest adsorption capacity has a zeolite of 1.7 mmol / g with a propane adsorption value of $R = 50\text{ mm Hg}$ in TsSK-2. The isotherm of adsorption on zeolite in TsSK-3 is slightly lower and also lower in TsSK-1. Thus, the mechanochemically activated zeolite that is part of the CSK has more adsorption capacity for propane than the zeolite introduced into the CSK without prior activation. The kinetic curves of propane adsorption on zeolites containing CSK drawn at $R = 2\text{ mm Hg}$ and $T = 292\text{ K}$ are shown in Figure 3.31. shown.

As can be seen from the figure, as at high pressure, the amount of adsorbed propane is higher in the initial pentacyl of YuKTs-1 than in YuKTs-2. The adsorption rate is also high in YuKT-1 and the time to establish the adsorption equilibrium in both zeolites is the same and is 6 minutes. The kinetic curves of activated zeolite in TsSK-2 and TsSK-3 are higher than in YuKTs-2, and the value of propane adsorption in TsSK-3 is 1.4 times higher than in YuKTs-2. and the value of propane adsorption in zeolite at TsSK-2 is almost twice that for YuKTs-2. Among all the samples studied, the highest rate of propane adsorption was observed in zeolite containing TsSK-2. The rate and amount of propane adsorbed on pentacyl containing TsSK-1 ($R = 2$ mm Hg) is the smallest of all the samples studied.



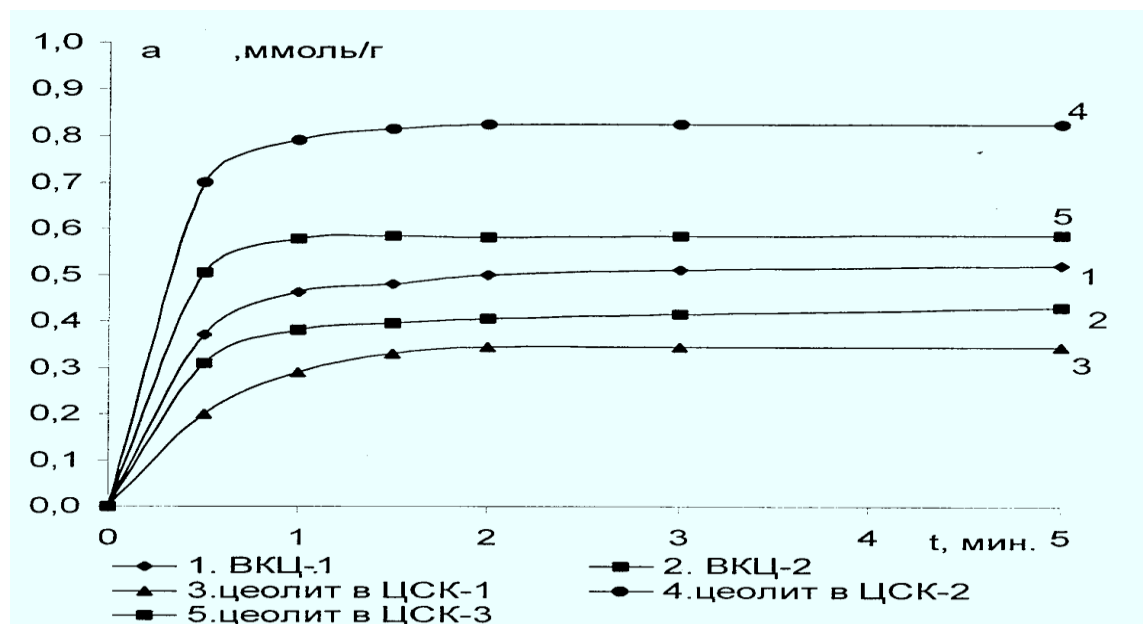
3.29 -image

Kinetic curves of propane adsorption in TsSK-2



3.30 -Picture

Isotherms of propane adsorption on zeolite in CSK ($T = 292$ K)



3.31 -Picture

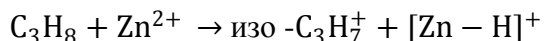
Kinetic curves of propane adsorption in primary YuKTs and pure zeolite in TSK ($T = 292$ K).

A comparison of the adsorption properties of zeolite catalysts with the structural properties showed that for CSK there is a clear relationship between the B coefficients of the Dubinin-Radushkevich equation and the amount of adsorbed propane: the higher the B coefficient, the more adsorbed the propane is. Pure zeolite in TsSK and TsSK ($TsSK -2 > TsSK -3 > TsSK -1$).

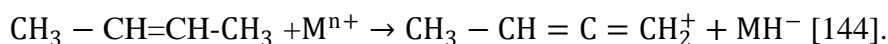
In practice, a similar sequence is obtained by comparing the adsorption properties of TsSK with the number of strongly acidic sites and their selectivity for arenas: $TsSK -2 > TsSK -3 > TsSK -1$.

Thus, the introduction of mechanically-chemically activated zeolite into the CSK leads to a change in its structural, adsorption and acidic properties, which in turn affects the CSK activity in the aromatization reaction.

Indeed, the results of calculating the rate of accumulation of aromatic hydrocarbons in continuous conversion showed that the aromatization of isobutane in Zn and Ga -pentacil is 9 and 12.5 times faster than in the normal forms, respectively [142]. Separation of a hydride ion from an alkane molecule in the presence of Zn^{2+} cations can occur according to the following scheme [120, 143]:

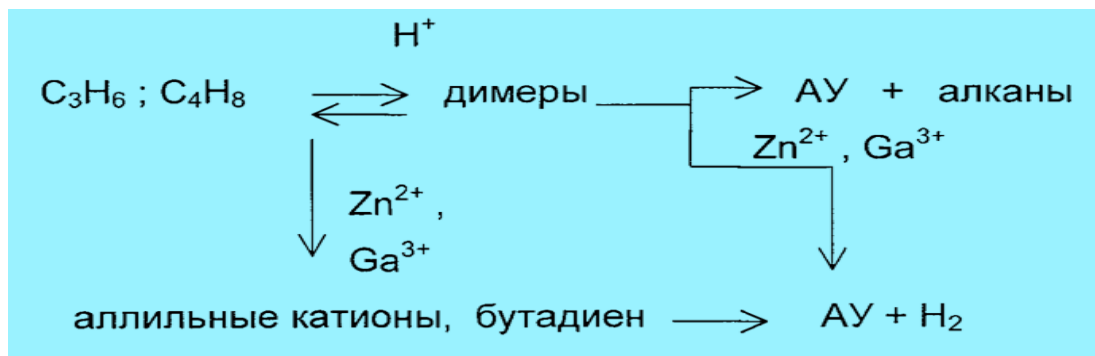


In this case, the cation Zn^{2+} acts as an acceptor of hydride ions. In addition to the first stage, dehydrogenation of saturated carbons, Zn and Ga, which are part of pentacil, is involved in the separation phase of the hydride ion from olefin molecules with the formation of allyl intermediates:



Based on the experimental data, a scheme for the conversion of lower olefins in pentacil modified with Zn and Ga was proposed.

[144]:

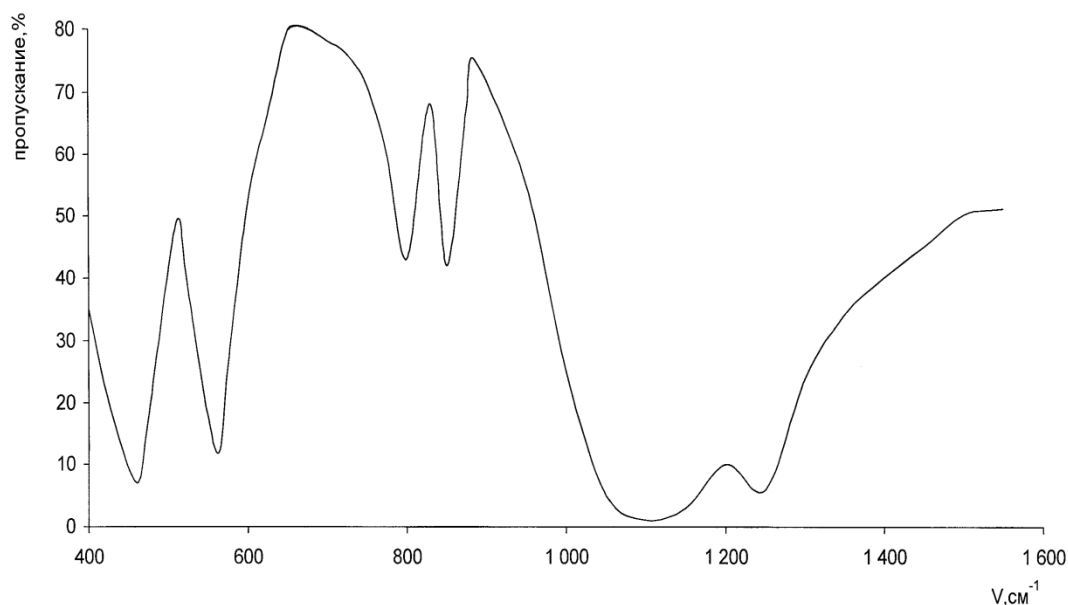


It follows from the scheme that aromatic hydrocarbons are formed as a result of the sequential separation of hydride ions from high-molecular-weight olefin molecules, as well as the interaction of two allyl structures with the simultaneous destruction of a hydrogen molecule.

IC spectroscopy and X-ray analysis were performed using physicochemical methods to study YuKTs: IR spectra of the studied zeolites (Figure 2.1) were recorded on a UR-20 spectrophotometer in the mid-wavelength part of the spectrum at 400-2000 cm^{-1} , where the absorption ranges were AIO₄ of the base. $[(SiO)_4]$ are the principal oscillations of the tetrahedron.

To do this, 1-2 mg of the sample and 400 mgKBr of potassium bromide are poured into a special ring placed in a mold, then the sample ring is inserted into the holder and placed on a spectrophotometer. Absorption lines in the observed spectrum can be divided into 2 types of oscillations [23, 171]:

1. $[(SiO)_4]$ oscillations within a tetrahedron, they are primary structural units. These oscillations do not reflect the specific properties of the zeolite structure.
2. Vibrations in the external connections of tetrahedrons. The second type depends on the zeolite structure, the ability to join in secondary structural units, as well as in structures that form entrance pores in the zeolite cavity. The first type of oscillations corresponds to oscillations at 1120 cm^{-1} 820 cm^{-1} and 470 cm^{-1} found in the whole zeolite spectrum. The strong absorption range at the peak of 1120 cm^{-1} is related to the antisymmetric oscillations of the $t(SiO)_4$ tetrahedron, while the 820 cm^{-1} length 3104 cm^{-1} tetrahedra represents the oscillations mainly involved []. The location of this group is affected by the Si / Al ratio in the zeolite content.

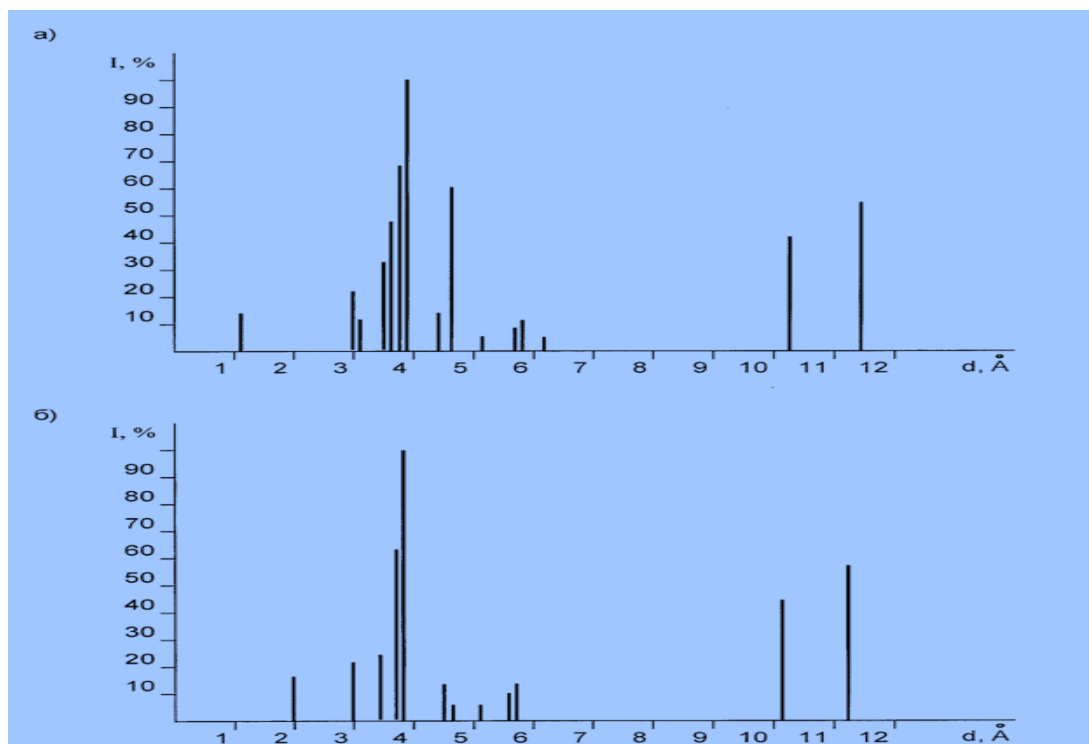


2.1 -Picture .

IR spectrum of zeolite synthesized ZSM -5 ($\text{SiO}_2 / \text{Al}_2\text{O}_3 = 70$).

As the composition of the al tetrahedron coordinated atoms increases, the assimilation ranges shift to the low frequency region [23s. 482]. Intensive absorption lines correspond to bending oscillations in a tetrahedron of 460 cm^{-1} $[\text{SiO}]_4$. The second type of vibration, which is sensitive to the nature of the dependence on the type of environment of the secondary connecting units in the tetrahedron, topology, and zeolite, corresponds to absorption 560 cm^{-1} lines. - The presence of strong absorption lines $1300\text{-}900$, 820 , $400\text{-}600 \text{ cm}^{-1}$ in the region of all spectra testifies to the fact that all samples belong to zeolites.

- that all tested specimens belong to the ZSM constructive type, since all IR spectra obtained include the absorption peaks line 560 cm^{-1} . the ratio of the optical absorption ranges to 560 and 460 cm^{-1} (I_{560} / I_{460}) [173], the crystallization rate of all studied samples was calculated: $\text{SiO}_2 / \text{Al}_2\text{O}_3$ for ZSM-5 zeolites with a ratio of 30, 50, 70, 100; crystallinity level 89, 2, respectively; 93.3; 91.5; 88.2% are equal. For the ZSM-11 catalyst ($\text{SiO}_2 / \text{Al}_2\text{O}_3 = 100$), the crystallization rate is 88.1%. There are no significant differences in IR spectra for ZSM-5 and ZSM-11 zeolites; therefore X-ray analyzes were performed to improve the structure of the zeolites in detail. X-ray analyzes (Mo-anode, Ni-filter) were performed using Dron-3. Processing of the diffraction lines of zeolites was carried out by comparing the distance between the planes (their position and relative intensity) with a sample of the corresponding lines and determining the distances and intensities of the lines (peaks) of the studied zeolite sample. Figure 2.2 shows the signs of linear X-ray diffraction of zeolites ZSM-5 and ZSM -11. Compared with the data in Table [23], the relationship between the relative intensity of the line and the distance between the planes ($d, \text{\AA}$) made it possible to determine the structural types ZSM -5 and ZSM -11.



2.2-image.

Signs of X-ray diffraction of synthesized zeolites noted

(*a*- ZSM -5; *b*- ZSM -11).

The marked diffraction characteristics of these samples are that for ZSM-5 there are three intensive lines in the region of small plane distances (d , Å: 3.84; 3.74; 3.62). There are only two intensity lines for the zeolite ZSM-11 (d , Å: 3.86; 3.73). The crystals of ZSM-11 zeolite differ from the crystals of other pentacycls by more perfect symmetry, with fewer lines in their diffractogram. VTK fractions, C₉₊ hydrocarbons, naphthalene and methylnaphthalene. C₂-C₄ alkane conversion products were analyzed using gas chromatography on a chromium chromatograph with a thermal conductivity detector. Analysis of gaseous products - in a column filled with Al₂O₃ (3) (0.25-0.5 mm, column length - 4 m, inner diameter - 3 mm), in the temperature programming mode from 298 to 423 K, with heater, speed 12 degrees / min. Carrier (He) gas velocity - 50 cm³ / min. The chromatogram of gaseous products is shown in Figure 2.5.

Liquid hydrocarbons were analyzed on a S2 + base at a temperature of 352 to 473 K in the programming mode at a rate of 12 OC / min and then in an isothermal mode at 473 K on a PFMS-4 stationary phase packed column. The chromatogram of gaseous products is shown in Figure 2.5.

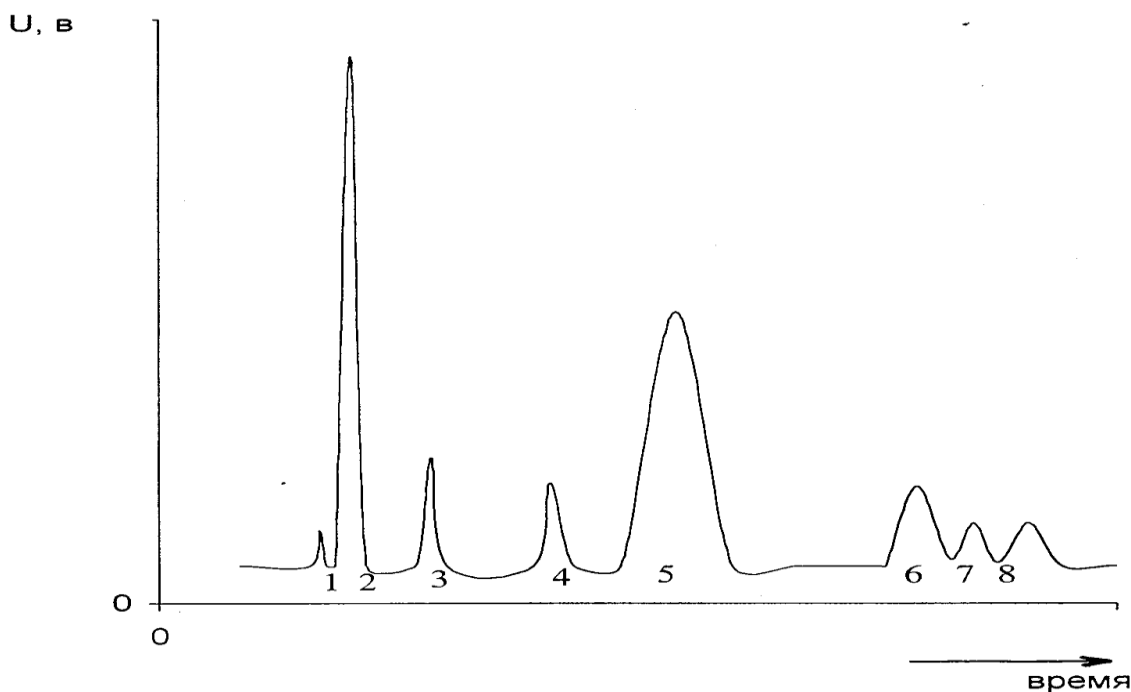


Figure 2.5 Chromatogram of gaseous products of alkane conversion S2 -S4

1. hydrogen 2. methane 3. ethane 4. ethylene 5. propane
6. propylene 7. Butane 8. Butylene

Carrier gas (He) velocity - 4.5 cm³ / min. The chromatogram of the liquid products is shown in Figure 2.6. Quantitative analysis of reaction products was performed using the internal optimization method [175]. The calculation consisted of converting half-width products to 100% of the height of all peaks of the chromatogram.

$$C_i = \frac{(k_i h_i I_i)}{(\sum k_i h_i I_i)} \times 100\% \quad C_j = \frac{(k_j h_j I_j)}{(\sum k_j h_j I_j)} \times 100\%$$

C_i is the concentration of i-components in the gas phase, % by weight;

S_j - j is the concentration of components in the liquid phase, % by weight;

i, j are half-width peaks

h_i, j - high peaks

where j is the coefficient determined by the sensitivity of the detector to a particular component.

In the calculation, we used the detector sensitivity correction factors given in [176]. The experimental data are as follows.

- 1) Calculate the mass of gas formed as a result of the reaction:

$$m = \frac{VxMr}{22,4}$$

V-Volume of gas

Mr- Molar mass of gas

22.4-Volume of gas under normal conditions

The mass of liquid hydrocarbons was determined by weighing the products formed at the end of each experiment. m_j can also be calculated using the following formula:

$$m_{ж} = V_{ж} \rho_j$$

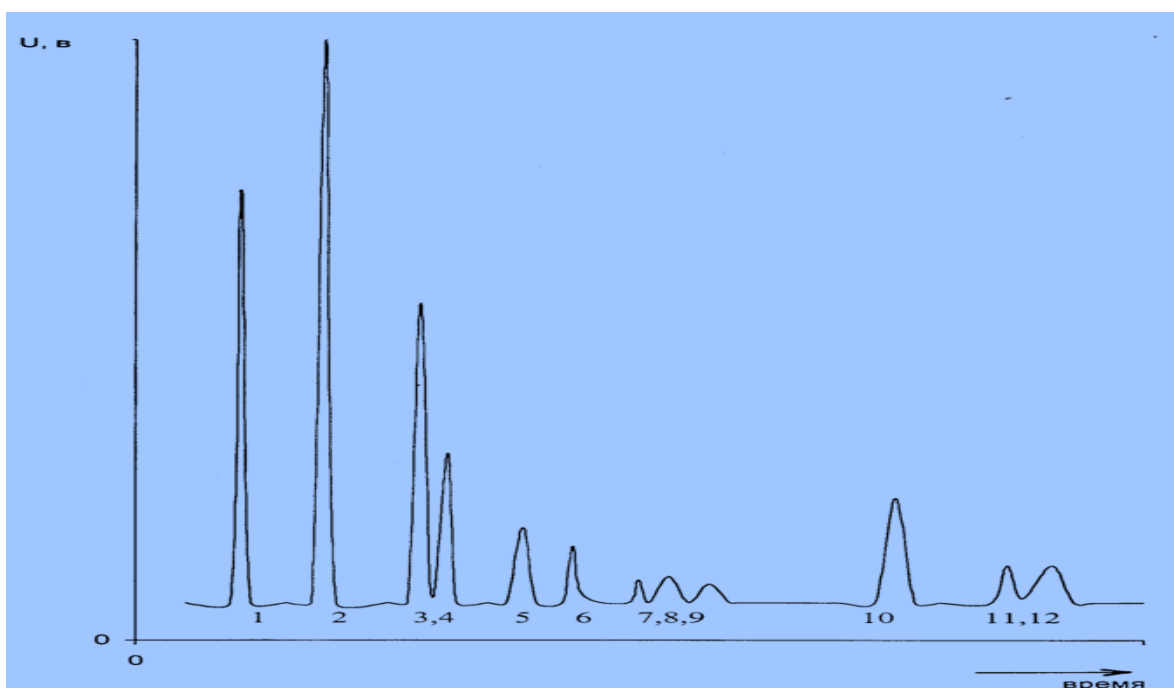
V_j = volume of liquid hydrocarbons cm^3

ρ_j = average density, g / cm^3

$V_j = S d_j p_j$

d_j = part of a large component

ρ_j = component density g / cm^3



1. benzene
2. toluene
3. m, p -xylene
4. o-xylene
5. methylethylene
6. pseudocumole
7. m-diethylbenzene
8. p-diethylbenzene
9. 1,2-dimethyl-3-ethylbenzene
10. naphthalene
11. α -methyl naphthalene
12. β -methyl-naphthalene

Figure 2.6 - S2 -S4 alkane conversion and chromatogram of liquid products

Mass fraction of gaseous products:

$$dr = m_2 / (m_r + m_{ж})$$

Mass fraction of liquid hydrocarbons: $d_j = 1 - dr$

Component concentration in the amount of hydrocarbons: $C_{-}(i) = d_{-r} C_{-}(I)$

j-component concentration of hydrocarbons: $S_j = d_j C_{-}^i$

The conversion rate (X) is calculated according to the following formula:

$$X = \frac{(M - m_{\max})}{M} \times 100\%$$

M is the total concentration of reaction products;

product - the total concentration of propane and butane in the reaction products;

mchish - the total concentration of ethane, propane and butane in the raw material. component selection is calculated according to the formula i, j [177-179]:

$$S_{i,j} = m_{i,j} / M_{\text{олинди}}$$

$m_{-}(i, j)$ - concentration of component i, j in reaction products,

M_{olindi} is the concentration of the converted raw material

Output i, j component (A): $A = S_{-}i \times X$

Table 3.1-8 | $[\text{SiO}]_{-2} / [\text{Al}]_{-2}$ Transformation of alkane mixture in high silica zeolite decanted by ZSM -5 with $O_{-3} = 70$.

Ҳарорат К	73	23	73	23	73	73	73	73	73
Ҳажмий тезлик $V_{\text{ч}^{-1}}$	00	00	00	00	00	0	5	00	50
Конверсия, %	7	4	7	5	7	6	1	7	4
Селективлик масса %									
Водород						2			
Метан	5	4	1	6	9	8	5	1	9
Этан	3	6	2	0	7	5	5	2	7
Этилен			0					0	
Пропилен					,5				
Бутен									
Бензол				,5	0	,5	3		

Толуол	0		1	0		0	5	1	0
Ксилол		,5					0		
Алкилбензол									
Нафталин углеводородлар									
C ₁ -C ₂ алканлар	9	1	3	6	6	3	0	3	7
C ₂ -C ₄ алкенлар	9	5	5	3	3			5	9
C ₆ -C ₁₂ аренлар	5	1	0	9	8	1	8	0	4
C ₆ -C ₁₂ чиқадиган аренлар	2	8	6	7	7	0	4	6	8
C ₂ -C ₄ чиқадиган алкенлар		2	3	2	3			3	4

CONCLUSION

1. The conversion reaction of a mixture of alkanes containing C₂H₆ = 2.2; C₃H₈ = 73.7; N-S₄N₁₀ = 24.1%. In high-silicate zeolite catalysts with the structure ZSM-5 ([SiO]₂ / [Al]₂ O₃ = 30, 50, 70 and 100) and ZSM-11 ([SiO]₂ / [Al]₂ O₃ = 100), the catalytic contacts the relationship between their structural and acidic characteristics and their activity in the formation of conversion products was studied.

2. In this process, the effect of technological parameters (reaction temperature and volumetric rate) on the activity and selectivity of zeolite catalysts was studied.

3. All used YuK zeolite catalysts are in N-form state. The results of the conversion of a mixture of low molecular weight alkanes with [SiO]₂ / [Al]₂ O₃ = 70 in ZSM-5 zeolite are given in Table 3.1.

4. With a significant yield of liquid products, the change of raw material begins at a temperature of 673 K. At this temperature, the conversion rate of low molecular weight alkanes [S]₂-S₄ is 47%. The reaction produces gaseous products: methane, ethane, ethylene, propylene, butene and liquid catalysis: benzene, toluene, xylenes (BTC fraction), alkylbenzenes, naphthalene and alkyl naphthalenes. The selectivity for the formation of aromatic hydrocarbons (S_{AY}) at a temperature of 673 K and $v = 100 \text{ s}^{-1}$ is 25.4%, alkenes [S]₂-S₄ 19.1% by weight. An increase in the reaction temperature from 673 K to 873 K leads to an increase in the conversion rate, while at 873 K the conversion reaches 97%. An increase in the selectivity of the formation of benzene and naphthalene hydrocarbons is also observed.

5. As a result of the work carried out, it was found that the role of the meso-porous structure of the matrix in the CSK is not limited to the function of "transport".
6. The introduction of the matrix leads to an increase in the size and volume of the zeolite pores, thereby increasing the reactive penetration of the acidic centers located inside the zeolite pores.
7. The close connection of the "zeolite-matrix" in the macropores of TSSK creates conditions for full use of the specific properties of zeolite in catalytic conversion.

REFERENCES

1. Recent progress in methane dehydroaromatization: from laboratory curiosities to promising technology / S. Ma, X. Guo, L. Zhao, S. Scott, X. Bao // *J. Energy Chem.* – 2013. – V. 22. – № 1. – P. 1–20.
2. Spivey J.J., Hutchings G. Catalytic aromatization of methane // *Chem. Soc. Rev.* – 2014. – V. 43. – P. 792–803.
3. Direct conversion of natural gas to higher hydrocarbons: a review // S. Majhi, P. Mohanty, H. Wang, K.K. Pant // *J. Energy Chem.* – 2013. – V. 22. – P. 543–554.
4. Металлцеолитные катализаторы дегидроароматизации метана // Н.А. Мамонов, Е.В. Фадеева, Д.А. Григорьев, М.Н. Михайлов, Л.М. Кустов, С.А. Алхимов // *Успехи химии.* – 2013. – Т. 82. – № 6. – С. 567–585.
5. Файзуллаев Н. И., Туробжонов С. М. Метан ванефтнингйўлдошгазлариникаталитикароматлаш // *Кимёвакимётехнологияси.* 2015. – No. 2. – Б. 3–11.
6. Catalytic chemistry for Methane Dehydroaromatization (MDA) on a bifunctional Mo/HZSM5 catalyst in a packed bed / C. Karakaya, S.H. Morejudo, H. Zhu, R.J. Kee // *Ind. Eng. Chem. Res.* – 2016. – V. 55. – P. 9895–9906.
7. Methane dehydroaromatization by Mo/HZSM5: Monoor bifunctional catalysis? / N. Kosinov, F.J.A.G. Coumans, E.A. Uslamin, A.S.G. Wijkema, B. Mezari, E.J.M. Hensen // *ACS Catal.* – 2017. – V. 7. – № 1. – P. 520–529.
8. Дергачев А.А., Лapidус А.Л. Каталитическая ароматизация низших алканов // *Рос.хим. журн. (Журн. Рос. хим. об-ва им. Д.И. Менделеева).* 2008. Т. LII. № 4. С. 15–21.
9. Ахметов А.Ф., Каратун О.Н. Модифицированные пентасилсодержащие катализаторы для ароматизации углеводородных газов // *Химия и технология топлив и масел.* 2001. № 5. С. 33–36.
10. Victor de O. Rodrigues, Arnaldo C. Faro Junior. On catalyst activation and
11. reaction mechanisms in propane aromatization on Ga/HZSM5 catalysts // *Applied Catalysis A: General* 435–436. 2012. Pp. 68–77.
12. Дергачев А.А., Лapidус А.Л. Превращения низкомолекулярных алифатических углеводородов на цеолитных катализаторах // *Газохимия.* 2008. № 4. С. 16–20.

13. Восмери́кова Л.Н., Волы́нкина А.Н., Восмери́ков А.В., Зайко́вский В.И. Ароматизация этана и пропана на металлосодержащих цеолитах структурного типа ZSM-5 // НефтеГазоХимия. 2015. № 1. С. 37–41.
14. Козлов А.М., Худяков Д.С., Лapidус А.Л., Дергачев А.А. Ароматизация пропан-бутановой фракции на пентасиле, модифицированном солями цинка // Технологии нефти и газа. 2011. № 1. С. 7–10.
15. M. Tian, T.Q. Zhao, P.L. Chin, B.S. Liu, A.S.-C. Cheung, Methane and propane co-conversion study over zinc, molybdenum and gallium modified HZSM-5 catalysts using time-of-flight mass-spectrometry // Chemical Physics Letters 592. 2014. Pp. 36–40.
16. Fayzullayev N.I., S.M.Turobjonov. Catalytic Aromatization of Methane // International Journal of Chemical and Physical Science. -2015. -Vol. 4, No-4. P 27-34
17. Fayzullayev N.I., B.Sh. Shukurov., A. Normuminov. Kinetics and Mechanism of the Reaction of Catalytic Dehydroaromatization of Methane // Petroleum Science and Engineering. India. -2017; N6: 36-42pp.
18. Файзуллаев Н. И., Туробжонов С. М. Метан ванефтнингйўлдошгазлари-ни каталитикароматлаш // Кимёвакимётехнологияси. 2015. – No. 2. – Б. 3–11.
19. Fayzullaev N. I., Shukurov B. Sh. Catalytic aromatization of methane with non-mo-contained catalysts //Austrian journalof technical andnatural sciences. № 7–8. - 2018. –PP-73-80.
20. N. I. Fayzullaev., B. Sh. Shukurov., A. O'. Normuminov. Kinetics and mechanism of the reaction of catalyticdehydroaromatization of methane// International Journal of Oil, Gas and Coal Engineering. 2017; 5(6): 124-129. <http://www.sciencepublishinggroup.com/j/ogce>. doi: 10.11648/j.ogce.20170506.11